Indian Journal of Experimental Biology
Vol. 61, April 2023, pp. 252-264
DOI: 10.56042/ijeb.v61i04.179

Autophagy in antitumor activity of aloin for breast cancer cells compared with doxorubicin

Emad K. Ahmed[1]*, Asmaa K. El-Gendy[1], Hala El-Tantawi[2], Mahmoud N. El-Rouby[3], Mahmoud M. Said[1], Hala M. Ghanem[1] & Amr Y. Esmat[1]

[1]Department of Biochemistry; [2]Department of Zoology, Histology Division, Faculty of Science, Ain Shams University, Cairo, Egypt
[3]Department of Cancer Biology, National Cancer Institute, Cairo University, Egypt

Received 05 February 2022; revised 17 February 2023

Breast cancer is the most commonly diagnosed cancer and is one of the leading causes of cancer mortality in women worldwide. Natural product compounds have attracted significant attention for their potent effects against human cancers. Aloin, a natural phytochemical anthraquinone glycoside extracted from *Aloe* sp., has been previously reported for its antitumor activity. Autophagy is a highly conserved process that mediates the degradation of dysfunctional cellular components, such as senescent proteins and organelles. In the present study, we verified the involvement of autophagy in tolerance to aloin, especially in breast cancer cells with negative estrogen receptors, and as an alternative pathway to promote cell death in cells expressing mutant p53 status, which often limits the efficacy and accounts for resistance to chemotherapy. We studied the effect of aloin on 2 types of breast cancer cell lines, estrogen receptor-positive (T47D) and triple negative (MDA-MB231), and compared to an anthraquinone analog, doxorubicin (Dox) as a reference compound. Aloin inhibited the cell growth of both T47D and MDA-MB231 cancer cells, in a time- and dose-dependent manner with a more pronounced effect in the 72 h exposure regimen, and in the ERα+ breast cell line. The autophagic activity of aloin was emphasized by the formation of autophagosomes and autolysophagosomes, as early and late autophagic compartments, respectively, as well as the accumulation of acidic vesicular organelles in the tumor cells. Also, upregulation in the protein expression of some marker genes of autophagy such as beclin 1 and LC3BII/LC3I, and conversely down-regulation in p-mTOR and p62 was recorded. The results suggest that autophagy can be regarded as one of the mechanistic modes of aloin cytotoxicity in breast cancer cells that evade apoptosis through genetic mutations in p53.

Keywords: *Aloe vera*, Chemosensitivity, Estrogen receptor.

Breast cancer is the most common cancer among women worldwide. In the United States of America, it is the most commonly diagnosed cancer in women accounting for about 30% of all new cancer cases in women each year. It is one of the leading causes of cancer related deaths in women, second only to lung cancer and it is estimated that about 13% of the total population of women in US may develop invasive breast cancer[1]. Two common subtypes are well-recognized for breast cancer and differentiated according to the status of estrogen receptor: Estrogen receptor positive (ERα+) and triple negative breast cancers (TNBC). The ERα+ are largely well-differentiated, less aggressive, with good prognosis and appreciably responds to hormonal therapy. On the other hand, the TNBC lack estrogen receptor, progesterone receptor and epidermal growth factor-2 receptor (ER−, PR− and HER2−), poorly differentiated, aggressive in behaviour, and with worst prognosis associated with poor outcome[2]. Chemotherapy remains the standard of care for TNBC treatment, though, patients frequently develop resistance[3]. To overcome chemoresistance in cancer, the researchers look towards nature for novel lead structures for development of improved chemo-therapeutics for alternative molecular targets or mechanisms especially in patients who suffer from defects in apoptosis-regulatory genes[3].

For years, apoptosis (type I programmed cell death) was treated to be the principal mechanism by which chemotherapeutics agents kill cells. As an alternative route of cell death, autophagy (type II programmed cell death, ATG) is emerging as an important target for new anticancer drugs[4,5]. However, it remains controversial whether ATG is tumor suppressive (through cell cycle arrest, promoting genome and organelle integrity, or inhibition of necrosis and

*Correspondence:
Phone: +202 1148839844
E-Mail: emad.ahmed@sci.asu.edu.eg

inflammation), or oncogenic (by promoting cell survival in the face of spontaneous or induced nutrient stress, or by facilitating oncogene-induced senescence or protecting tumors against necrosis and inflammation)[6]. Study of anthraquinones in cancer-related topics is an auspicious endeavor, and evaluating their role in ATG could lead to a better understanding of their cytotoxic effects. Therefore, further investigations should be done to understand and clarify how autophagy relates to cancer therapy, how the autophagy pathway can be targeted and regulated by chemotherapeutics, and how the activity of ATG pathway can be monitored and quantified during cancer therapy.

Aloe vera (L.) Burm.f. is a perennial succulent medicinal plant that has been used in folk medicine for thousands of years. The preclinical studies over the last couple of decades uncover the potential therapeutic activities of *Aloe* plant and its bioactive compounds in many pharmaceutical products, functional foods, and cosmetics[7]. Aloin is one of the main natural bioactive ingredients of *A. vera*. It is an anthraquinone glycoside with an empirical formula of aloin is $C_{21}H_{22}O_9$, which is supported by the formulation 10 β-D-glucopyranosyl-1,8- dihydroxy-3-hydroxymethyl-anthracene-9-one. Aloe-emodin showed its efficacy to inhibit proliferation and to induce apoptosis, *in vivo* and *in vitro*, in many types of cancerous cells by various mechanisms[8]. In our previous studies, we reported the antitumor activity of aloin against experimental murine tumors (ascites and solid Ehrlich carcinoma)[9,10], with no detrimental side effects on the host metabolism[11]. Further studies in our lab have shown the cytotoxicity of aloin against different types of human cancer cell lines, such as breast and ovarian adenocarcinoma cell lines[12,13]. We have also demonstrated that there was no cardiotoxicity for the repeated treatment of normal rats with the maximum tolerated dose of aloin (50 mg/kg bw) due to its strong antioxidant and scavenging activities for free radicals and reactive oxygen species[14], as well as its strong iron chelating activity[15].

In the present study, we propose to investigate the cytotoxic effect of aloin against two subtypes of breast cancer cell lines, ERα+(T47D) and TN (MDA-MB231), compared to its anthraquinone analog, doxorubicin (Dox) as a reference compound. Further, we investigated contribution of the ATG process to the antitumor activity or tolerance of aloin.

Materials and Methods

Chemicals

Aloin (M.W. 818.4) was provided in a pure form from MacFarlan Smith LTD (Edinburgh, Scotland). Adriamycin hydrochloride (M.W. 579.5) was provided in the form of a red lyophilized powder from Pharmacia S.P.A. (Milan, Italy). RPMI-1640/ L-glutamine medium, and fetal bovine serum (FBS) were from Gibco (Thermo Fisher Scientific, USA). DMEM/L-glutamine medium and Trypsin/EDTA (1×) were from Biowest (South Africa). Penicillin/ Streptomycin mixture (1×) was from Biochome AG (Germany). Dimethyl sulfoxide (DMSO) and Phosphate-buffered saline (PBS) were from Sigma-Aldrich (Germany). 3-(4,5-dimethylthiazol-2-yl)-2,5-diphenyltetrazolium bromide (MTT), absolute methanol, sterile tissue culture flasks (75 cm^2), Petri dishes (58 cm^2), and 96-well microtiter plates were provided from Thermo Fisher Scientific (USA).

Cell lines and cell culture

Two human breast cancer cell lines were used in this study; T47D (ERα+, PR+ and HER2-, mutant p53) (CAT. No HTB-133™) and MDA-MB231 (ERα-, PR-, HER-2-, mutant p53) (CAT. No HTB-26™) (ATCC, USA). T47D cells were cultured in RPMI-1640/L-glutamine medium, whereas MDA-MB231 cells were cultured in DMEM/L-glutamine medium in a humidified 5% CO_2 incubator at 37°C. Both media were enriched with 10% heat inactivated FBS and 1% penicillin/streptomycin mixture. Sub-culturing of exponentially growing cells was carried out weekly using trypsin/EDTA.

Compounds preparation

A stock solution of aloin (2 mg/mL) was freshly prepared in sterile warmed distilled water (50°C). The solution was sterilized by filtration through 0.22 µm filter (Sigma-Aldrich, St. Louis, MO, USA). Two sets of serial dilutions were prepared from aloin stock solution in respective complete growth media for treatment of T47D cells (20, 40, 60, 80 and 100 µg/mL) and MDA-MB-231 cells (20, 80, 100, 150, 200, 300 and 400 µg/mL). Alternatively, two sets of concentrations were prepared from Dox stock solution (2 mg/mL) in RPMI-1640 complete growth medium for T47D treatment (0.05, 0.1, 0.15 and 0.2 µg/mL), and incomplete DMEM culture medium for MDA-MB231 treatment (0.01, 0.1, 1 and 10 µg/mL).

Chemosensitivity studies

The cytotoxic effects of aloin and Dox against tumor cell proliferation of T47D and MDA-MB231

cells were assessed by two experiments, MTT and clonogenic assays.

MTT assay:

For each cell line, exponentially growing cells were enzymatically detached and inoculated into 96-well microplates at a density of 30,000 cells/well, and then allowed to attach for 24 h under the previous specified conditions. Following attachment, cells were exposed to increasing concentrations of aloin and Dox (positive control) and incubated for 24 and 72 h in triplicate independent experiments. At the end of exposure periods, the media were removed, and cell viability was determined by MTT assay[16]. The percentage of cell viability was calculated by multiplying the ratio absorbance of the sample versus the control by 100. Drug IC_{50} value defined as the half maximal inhibitory concentration that reduces cell viability by 50% was deduced for aloin and Dox in the 72 h exposure regimen in both cell lines from the nonlinear regression line in the dose-response inhibition curves using GraphPad Prism software.

Clonogenic assay:

A free single tumor cell suspension was prepared at a density of 6000 cells/mL. Aliquots of cell suspension (5 mL) were then transferred to 75 cm^2 tissue culture flasks and incubated in a humidified CO_2 incubator at 37°C for 24 h. After cell attachment, the culture medium was decanted and replaced with 5 mL of fresh complete growth medium in the control flasks and with 5 mL of fresh complete growth medium containing the different concentrations of aloin or Dox, and then re-incubated for 24 and 72 h, respectively. After incubation, the media were aspirated and the cells were trypsinized, and then collected in 15 mL falcon tubes containing fresh complete growth medium. The tubes were centrifuged, and then the cell pellets were re-suspended in 4 ml of fresh complete growth medium. The viable cell numbers were counted by trypan blue exclusion method, and then the cells were diluted with the complete growth medium to 1000 cells/mL. A volume of 1 mL cell suspension was transferred to three Petri dishes for control and for each compound concentration followed by the addition of 3 mL complete growth medium. The dishes were incubated in a humidified 5% CO_2 incubator at 37°C for 10 days, during which the drug-free growth medium was replaced every 72 h. At the end of the incubation period, the growth medium was decanted, and the colonies were fixed in absolute methanol for 20 min, then stained with 2% crystal violet and counted using a stereomicroscope (Olympus, Japan). The number of tumor colonies was scored by counting the cell aggregates consisting of at least 50 cells (>5 generations). At least 200 tumor cell colonies per flask were required in the control Petri dish to assure an adequate range for measurement of the compound effect. The mean tumor colonies count for control was taken as 100% survival (0% inhibition), and the percentage of inhibition of colony formation (%ICF) in compound-treated Petri dishes was calculated as follows: $\%ICF = (C - T)/T \times 100$, where C = mean of colonies count in control and T = mean of colonies count in treated cells.

Monitoring of autophagy process

Transmission electron microscopy (*TEM*)

TEM was used as a powerful technical approach for investigating the process of ATG and monitoring of ultrastructural morphology of autophagic compartments in the cells. After cell plating, media were discarded and the cells were washed with PBS, and then treated with fresh media containing IC_{50} values of aloin or Dox for T47D and MDA-MB231. The plates were incubated in a humidified 5% CO_2 incubator at 37°C for 24 and 72 h in independent experiments. At the end of the exposure period, the cell pellets were collected and prepared for primary fixation using 3% glutaraldehyde solution for 2 h at 4°C, after which were washed 3 times with PBS. Post fixation step was followed using 0.5% osmium tetroxide in phosphate buffer for 1.5 h at room temperature (25°C), after which cells were washed twice in PBS, then dehydrated in a graded dilution series of ethyl alcohol (50, 70, 90, 96 and 100%) at RT. Infiltration was done using 1,2 propylene oxide twice, each for 15 min. The packed cells were embedded in a mixture of propylene oxide and epoxy resin (EMbed-812 resin kit, Electron microscopy Sciences, England) and transferred into inverted polyethylene embedding capsule with conical tip (BEEM capsule size 3, Electron microscopy Sciences, England), and then left to polymerize at 60°C overnight. After polymerization, the blocks were trimmed and about 1.0 µm sections were cut, mounted on a glass slide, stained with 1% toluidine blue solution, and examined under light microscope as a guide in trimming the block face to an area suitable for ultrathin sectioning. Using ultramicrotome (Leica, Germany), ultrathin sections were cut at 75-90 nm and placed on copper grids (2 grids), and then stained

with 2% uranyl acetate and 0.4% lead citrate to be examined by TEM (Jeol-JEM-100s, Japan) at a magnification power of × 2000-8000.

Detection of acid vesicular organelles (*AVOs*) *by confocal fluorescence microscopy*

Acridine orange is a cell-permeable versatile fluorescence dye that can be protonated and trapped in acidic vacuoles (lysosomes, endosomes, and autophagolysosomes), RNA and DNA in living cells, and fluoresce red. To perform the assay, cells were first plated to allow a monolayer formation. Culture media were then replaced with fresh media containing either no compound (control) or IC_{50} values of the tested drugs (aloin and Dox) for 72 h. At the end of the incubation period, media were aspirated, and cells were washed with PBS, and then stained with acridine orange at a final concentration of 1 µg/mL for 15 min at RT in the dark. The acridine orange was removed, cells were washed with PBS, and then fresh media were added. The fluorescence was examined by confocal laser scanning microscopy (Carl Zeiss, LSM- 710, Germany). The excitation laser was 488 nm and 543 nm, while emission filters were 523 nm and 640 nm for green and red fluorescence, respectively. Acridine orange-stained cells were imaged, in which the cytoplasm and the nucleus fluoresce green, whereas the AVOs fluoresce bright orange/red with intensity proportional to the degree of acidity and the volume of AVOs. Fluorescent micrographs were taken using an integrated ZEN Software version 2.3.

Quantification of acidic vesicular organelles (*AVOs*) *by flow cytometry*

The number of cells with increased AVOs was determined by flow cytometry. After exposure of the different breast cancer cells to IC_{50} values of aloin and Dox for 72 h, as previously mentioned, the culture medium was decanted, and cells were washed with PBS and then trypsinized. Following cell detachment, 5 mL of fresh complete growth medium were added, and cells were collected in a falcon tube, centrifuged at 200×g for 2 min, and then the supernatant was discarded. The cell pellets were re-suspended in 5 mL fresh complete growth medium and stained with acridine orange at a final concentration of 1µg/mL for 20 min at RT. Acridine orange was removed by centrifuging the tubes at 150×g for 3 min, and the cell pellet was then re-suspended in 1 ml of PBS. Green (FL-1-H, Fluorescein isothiocyanate (FITC) 510/530 nm) and red (FL-3-H, 650nm, Phycoerytrin-cyanine 5 (PC5) fluorescence emission from 10000-20000 cells illuminated with blue excitation light (488 nm) was acquired by CytoFLEX flow cytometer (Beckman Coulter, Life Sciences, USA) and analyzed by integrated CyExpert Software.

Protein expression of autophagy markers by Western blot analysis

Cells were plated and incubated with IC_{50} values of aloin and Dox for 24 and 72 h in independent experiments as previously mentioned, and then adherent cells were harvested by scraping in ice-cold PBS. Three plates were set up for control and each drug in each cell line. The pooled cell suspension was centrifuged at 3000 rpm for 3 min. at 4°C, and the supernatant was discarded. Cells were lysed in ice-cold lysis buffer (50 mM Tris-HCl, pH 7.4, 150 mM NaCl, 1 mM EDTA, 1% Triton ×100) containing diluted protease inhibitor cocktail (×1000) (10 µL/mL lysis buffer). After three freeze/thaw cycles in liquid nitrogen, lysates were centrifuged at 10,000 rpm for 10 min at 4°C. Total protein concentration was determined in the cytosolic samples of the whole cell lysates by the method of Bradford[17] using a commercial assay kit (Biobasic Inc, Canada). Extracts were then diluted in lysis buffer to equal protein concentrations and stored at -80°C until analyzed. SDS-PAGE was performed according to Laemmli[18]. Proteins (50 µg) in sample buffer were heated at 90°C for 5 min. then loaded on 10% gels, electrophoresed, and electrotransferred onto polyvinyl difluoride membrane (PVDF) membranes. Transfer efficiency was routinely inspected by staining the membranes in Ponceau S. Nonspecific antibodies bindings were blocked by pre-incubation of the membranes for 1 h with Tris buffer (pH 7.4) supplemented with 0.3% Tween-20 and 3% bovine serum albumin. The membranes were then separately incubated with the following diluted polyclonal rabbit antibodies provided by Invitrogen (ThermoFisher Scientific, USA): p-AKT (Ser-473) (CAT. No PA5-85513, MW 60KDa), p-mTOR (Ser2481) (CAT. No PA5-77981, MW 289KDa), LC3B (CAT. No PA1-16930, MW 17-19KDa), beclin 1(CAT. No PA5-96649, MW 60 KDa), SQSTM1/sequestome (p62) (CAT. No PA5-20839, MW 62KDa) and β-Actin (CAT. No PA1-16889, MW 42KDa). The membranes were furtherly incubated for 1 h at 4°C with goat horseradish peroxidase-conjugated secondary antibody IgG (CAT. No 31460). The membranes were then washed thrice (PBS, 0.1% and Tween-20), the peroxidase-catalyzed

reaction was visualized with enhanced chemiluminescence (Clarity™ Western ECL substrate, BIO-RAD, USA), and the chemiluminescent signals were captured using a CCD camera-based image. Image analysis software was used to read the band intensity of the target proteins against control sample after normalization to β-actin on the digital Chemi Doc MP imager (Bio-Rad, USA).

Statistical Analysis

The Shapiro-Wilks test for normality showed that all data were normally distributed (P >0.05)[19]. Comparison was made using one-way analysis of variance (ANOVA). In case of a significant F-ratio, Bonferroni's test for multiple comparisons was used to evaluate the statistical significance between treated groups at P <0.05 level of significance. All the statistical analysis was done using Statistical Package for Social Science (SPSS) version 20.0 (SPSS Inc., Chicago, IL, USA).

Results

Effect of aloin on cell viability of breast cancer cells

Dose-response curves of aloin showed that brief exposure (24 h) to aloin failed to attain 50% reduction in cell viability of T47D cells, whereas the continuous exposure (72 h) of aloin produced a significantly dose-dependent reduction in cell viability, which reached 45.81% at the highest dose level (100 µg/mL), compared to the control cells (Fig. 1A). On the other hand, treatment of T47D cells with Dox produced a significant reduction in cell viability attaining a minimum of 83 and 41% at dose 0.15 µg/mL after 24 and 72 h exposure, respectively, compared to the control cells (Fig. 1B). As for MDA-MB231 cells, MTT assay revealed that aloin reduced the cell viability in a time- and dose-dependent manner. A gradual reduction in cell viability was obtained, reaching a nadir of 55.6 and 42.35% at the highest aloin dose (400 µg/mL) in the 24 and 72 h exposure assay, respectively (Fig. 1C). On the other hand, Dox produced a significantly gradual reduction in cell viability, attaining a minimum of 89.52 and 30.87% at the highest dose (10 µg/mL) in the 24 and 72 h exposure regimens, respectively (Fig. 1D). It is worthy to note that the prominent effect of aloin and Dox was achieved in the 72 h assay in both types of breast cancer cells, from which the IC_{50} values of both drugs were calculated and found to be 75 and 0.1 µg/mL, respectively, for T47D cells, and 295 and 1.0 µg/mL, respectively, for MDA-MB231 cells (Fig. 2 A and B).

Effect of aloin on the clonogenicity of breast cancer cells

In parallel with MTT assay, exposure of T47D cells to aloin showed a time- and dose-dependent reduction in the number of tumor colonies, attaining a

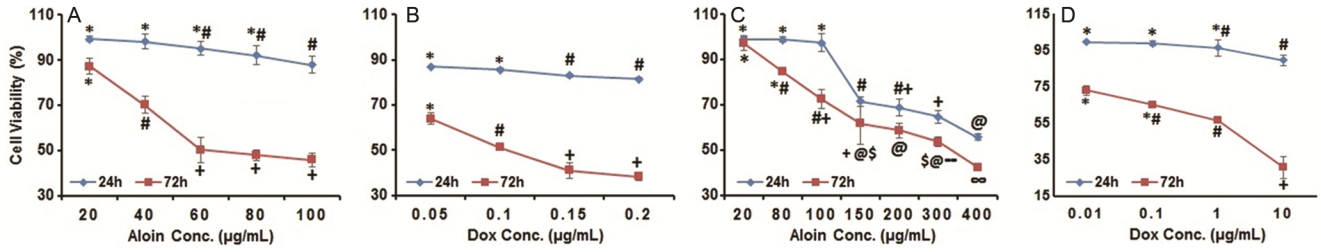

Fig. 1 — Dose-response curves of cytotoxicity of aloin and Dox in (A and B) T47D; and (C and D) MDA-MB231 cells. T47D cells were exposed to (A) aloin or (B) Dox @ 20-100 µg/mL and 0.05-0.2 µg/mL, respectively for 24 and 72 h. MDA-MB231 cells were treated with (C) aloin or (D) Dox @ 20-400 µg/mL and 0.01-10 µg/mL, respectively for 24 and 72 h. [Viable cells were detected by MTT assay and the % viability was determined as the ratio between treated and control cells. Similar symbols within the same data line denote insignificance (P >0.05). The data are represented as means± SD from three independent experiments]

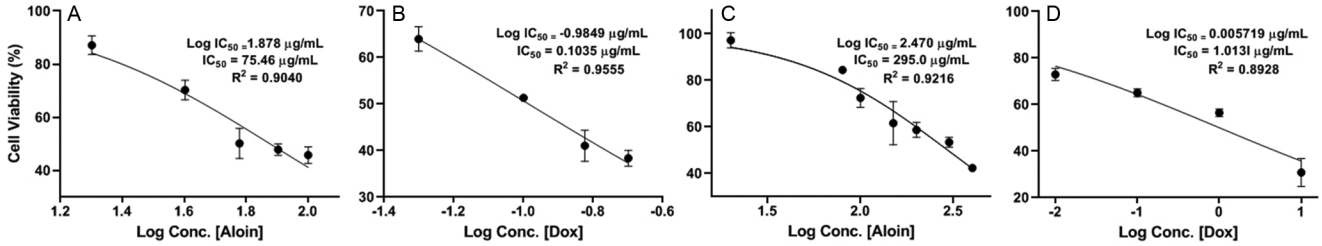

Fig. 2 — Plotting of % cell viability of (A and B) T47D; and (C and D) MDA-MB231 tumor cells *vs*. log concentrations of aloin and Dox which were used to calculate the half maximal inhibitory concentration (IC_{50} value) of aloin and Dox after 72 h exposure by GraphPad Prism software.

maximum %ICF of 71.8 and 100% at the highest dose level (100 µg/mL) in 24 and 72 h exposure regimens, respectively. The half inhibitory effect of aloin (53.62%) was recorded at dose 60 µg/mL in the 72 h exposure assay (Table 1). On the other hand, prolonged exposure of MDA-MB231 cells to aloin showed a gradual increase of % ICF, attaining the half maximal inhibition of tumor colonies (50.96%) at concentration 300 µg/mL. Alternatively, Dox treatment for 72 h exerted the highest %ICF of 95.11% at concentration 0.2 µg/mL in T47D cells, and 100% at 10 µg/mL in MDA-MB231 cells (Table 1).

Ultrastructure examination of aloin-treated breast cancer cells by TEM

TEM examination of control T47D and MDA-MB231 tumor cells revealed similar ultrastructural features; irregularity in shape with numerous surface microvilli, chromatin-condensed nucleus with prominent nucleolus, distinguishable mitochondria, and rough endoplasmic reticulum (Figs 3A and 4A). In general, the presence of time- and dose-dependent ATG features were prominent in the 72 h exposure regimen for both drugs and in both cell lines. T47D and MDA-MB231 cells treated with aloin for 24 h manifested a shrinkage of the nucleus (N), presence of various malformed, fragmented mitochondria (M), and moderate autophagic vacuoles. Also, double membrane autophagosomal vacuoles containing cellular parts were markedly appeared (Figs 3B and 4B). Continuous exposure of tumor cells to IC_{50} value of aloin induced the formation of autophagosomal vesicles in the cytosol manifested by the presence of electron-dense materials. Moreover, T47D cells treated with aloin for 72 h showed nuclear shrinkage, margination, and condensation of the chromatin (Figs 3D and 4D). On the other hand, exposure of T47D and MDA-MB231 cells to Dox for 24 h demonstrated

Table 1 — *In vitro* sensitivity of T47D and MDA-MB231 cells to aloin and doxorubicin

Dose of drugs (µg/mL)		24 h		72 h	
		No. of colonies	ICF %	No. of colonies	ICF %
T47D cells					
Control		418±15.6[a]	0	470±10.0[a]	0
Aloin	20	370±11.68[b]	11.5	335±15.0[b]	28.72
	40	340±13.58[b]	18.66	292±18.9[c]	37.87
	60	265±14.05[c]	36.6	217±16.6[d]	53.62
	80	194±12.90[d]	54.5	90±12.50[e]	80.85
	100	118±14.53[e]	71.8	ND[f]	100
Control		418±15.6[a]	0	470±10.0[a]	0
Dox	0.1	360±20.0[b]	13.88	401±11.5[b]	14.68
	0.1	232±6.5[c]	44.50	220±13.1[c]	53.19
	0.15	103±9.5[d]	75.84	80±5.0[d]	82.98
	0.2	40±4.5[e]	90.67	23±7.0[e]	95.11
MDA-MB231 cells					
Control		400±10[a]	0	418±17[a]	0
Aloin	20	373±12.6[a,e]	6.75	383±15.3[a,g]	8.37
	80	365±5[b,e]	8.75	373±6.4[b,g]	10.77
	100	355±5[b,e]	11.25	352±18.6[b,c,g]	15.79
	150	345±13.2[b,e]	13.75	318±17.6[c]	23.92
	200	283±17.5[c]	29.25	258±6.8[d]	38.28
	300	258±10.4[c]	35.5	205±5.0[e]	50.96
	400	205±5.03[d]	48.75	77±16[f]	81.58
Control		400±10[a]	0	418±17[a]	0
Dox	0.01	348±7.6[b]	13	321±8.08[b]	23
	0.1	248±7.2[c]	38	219±14.5[c]	47.5
	1	213±2.8[d]	46	103±9.5[d]	75.2
	10	ND		ND	

[Results are expressed as mean±SD of triplicate plates. ICF% represents the percentage of inhibition of colony formation. Different symbols within the same data column denote significance at $P<0.05$]

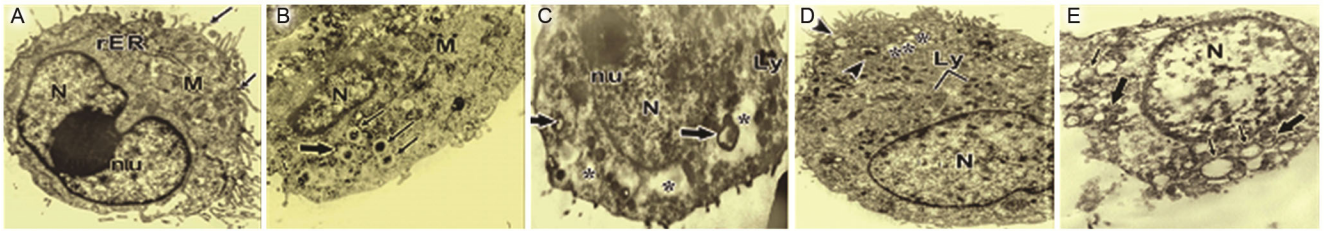

Fig. 3 — Transmission electron micrograph of (A) control T47D cells showing notched nucleus (N) with intended nuclear envelope, highly chromatic large nucleolus (nu), numerous microvilli (arrows) on the cell surface, many polymorphic mitochondria (M), and fragmented rough endoplasmic reticulum (rER) free of ribosomes dispersed in the cytoplasm; (B) T47D cells treated with aloin (75 µg/mL) for 24 h showed a shrinkage of the nucleus with various malformed and fragmented mitochondria, as well as marked double-membraned autophagosomes containing cellular parts (arrows); (C) T47D cells treated with Dox (24 h) showed a non-homogenous and degenerated euchromatin of the nucleus with eccentric nucleolus, autophagic vacuoles containing either degraded cellular components (asterisks) or partially degraded electron dense materials (arrows), and various lysosomal granules (Ly) in the cytoplasm; (D) T47D cells treated with aloin (75 µg/mL) for 72 h displayed thin-walled autophagolysosomes containing cellular debris (arrow head), remarkable autophagosomal vacuoles (asterisks) and numerous perinuclear lysosomes; and (E) T47D cells treated with Dox (72 h) showed a profoundly affected cell with a hypochromatic nucleus, marked increase of double-membraned autophagosomal vacuoles containing parts of the cytoplasm (thin arrows) as well as notable autolysosomes formed by fusion of some autophagosome vacuoles with lysosomes (thick arrows).

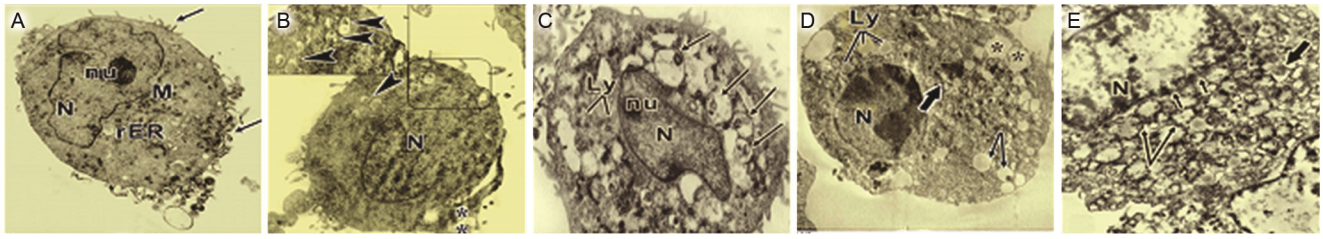

Fig. 4 — Transmission electron micrographs of (A) MDA-MB231control cells showing notched nucleus (N) with intended nuclear envelope, a highly chromatic large nucleolus (nu), cell surface microvilli (arrows), polymorphic mitochondria (M), and prominent rough endoplasmic reticulum (rER) within the cytoplasm; (B) MDA-MB231 cells treated with aloin (295 µg/mL) for 24 h showed a well-preserved nucleus, multiple autophagosomes including residual digested cellular parts (arrow head), and cytoplasmic vacuolation at the peripheral portion of the cell (asterisks); (C) MDA-MB231 cells treated with Dox (1 µg/mL) for 24 h showed the presence of many double-membraned autophagic vacuoles of different sizes enclosing fragmented parts of mitochondria and cytoplasmic components (arrows). Few lysosomes (LY) are also evident in the cytoplasm; (D) MDA-MB231 cells treated with aloin (295 µg/mL) for 72 h showed presence of lysosomes, formation of autolysosomal vesicles (asterisks), and many small autophagic vesicles (thick arrows). Some cytoplasmic vacuolations are evident (thin arrows); and (E) MDA-MB231 cells exposed to Dox (1 µg/mL) for 72 h showed a profoundly impacted cell with hypochromatic nucleus and disrupted nuclear envelope (small arrows). The cell consisted almost entirely of autophagic vesicles; some vesicles enclosed cellular debris (thin arrows). The fusion of lysosomes with some autophagic vesicles is also indicated (thick arrow).

a change in the size of cells, and the nuclei displayed a smooth surface lobulated with well-preserved nucleoplasm, while the nuclear envelope remained intact (Fig. 3C and Fig. 4C). The most prominent features were multiple lysosomes, as well as cytoplasmic membrane-bounded vesicles containing portions of the cytosol characteristic of ATG. After 72 h treatment with Dox, T47D and MDA-MB231 tumor cells showed a loss of distinct morphological features as a sign of ongoing degradation. The cytoplasm was almost filled with autophagic vacuoles containing-dense elements. Intracellular organelles were also reduced in number and ultrastructurally changed. Moreover, fusion of lysosomes with some autophagic vesicles manifested by the presence of autolysophagosomal vesicles filled with partially degraded materials was evident (Fig. 3E and Fig. 4E).

Detection and quantification of acidic vesicular organelles (AVOs) in aloin-treated breast cancer cells

Representative micrographs (Fig. 5) showed that T47D control cells emitted only green fluorescence, whereas aloin treatment (75 µg/mL) for 72 h induced the formation of an increased number of AVOs (autophagic cells) emitting punctate red fluorescence in T47D cells, which was augmented in Dox treatment (0.1 µg/mL). On the other hand, exposure of MDA-MB231 cells to aloin (295 µg/mL) for 72 h resulted in the accumulation of red-orange AVOs in their cytoplasm, while those treated with Dox (1 µg/mL) showed an ever-marked increase in AVOs (Fig. 5A). Interestingly, the MDA-MB231 control cells emitted green fluorescence with minimal red fluorescence (Fig. 5A). To quantify the development of AVOs, the acridine orange-stained cells were analyzed by flow cytometry, which measures the amount of light emitted in the red FL-3 channel that is directly correlated to the volume of cellular acidic compartments, i.e the autophagic cells in the cell population. The percentage of AVOs-containing cells in Dox treatment was almost double that in tumor cells treated with aloin (92.9 and 43.7%, respectively) (Fig. 5 B and C). Surprisingly, nearly half of MDA-MB231 control cells (48.7%) were positive for acridine orange stained-vesicular organelles (AVOs), which indicates the presence of autophagic cells. By contrast, the accumulation of AVOs was more pronounced in aloin- than in Dox-treated cells (70.7 and 61.2%, respectively), which indicates the induction of autophagic cell death by aloin and Dox (Fig. 5C).

Protein expression of ATG-regulated genes in aloin-treated breast cancer cells

Brief exposure (24 h) of T47D cells to aloin or Dox caused a variable increase in the protein expression levels of p-AKT (160 and 180%), beclin1 (50 and 40%), LC3I (52 and 108%) LC3II (190 and 310%), and their ratio LC3II/LC3I (90.8 and 97.11%, respectively), compared to their respective controls. The increase in the protein expression levels was augmented in T47D cells after prolonged exposure to aloin and Dox recording (290 and 350%), (260 and 202%), (136 and 156%), (370 and 390%) and (99.15 and 91.4%) for p-AKT, beclin 1, LC3I, LC3II, and LC3II/LC3I, respectively. Likewise, treatment of MDA-MB231 with aloin and Dox for 24h increased the protein expression of p-AKT (201 and 190%),

beclin 1 (57.4 and 77.2%), LC3I (401 and 509%), LC3II (240 and 420%) and LC3II/LC3I (158 and 224.5%), respectively. A more notable increase in the foregoing markers was noticed following aloin or Dox treatment for 72 h averaging (330 and 370%), (265 and 275%), (710 and 920%), (590 and 703%) and (233.7 and 199%), respectively. By contrast, both of T47D and MDA-MB231 tumor cells showed a mild to moderate repression in the protein expression of p-mTOR reaching 8 and 9% for aloin, as well as 42 and

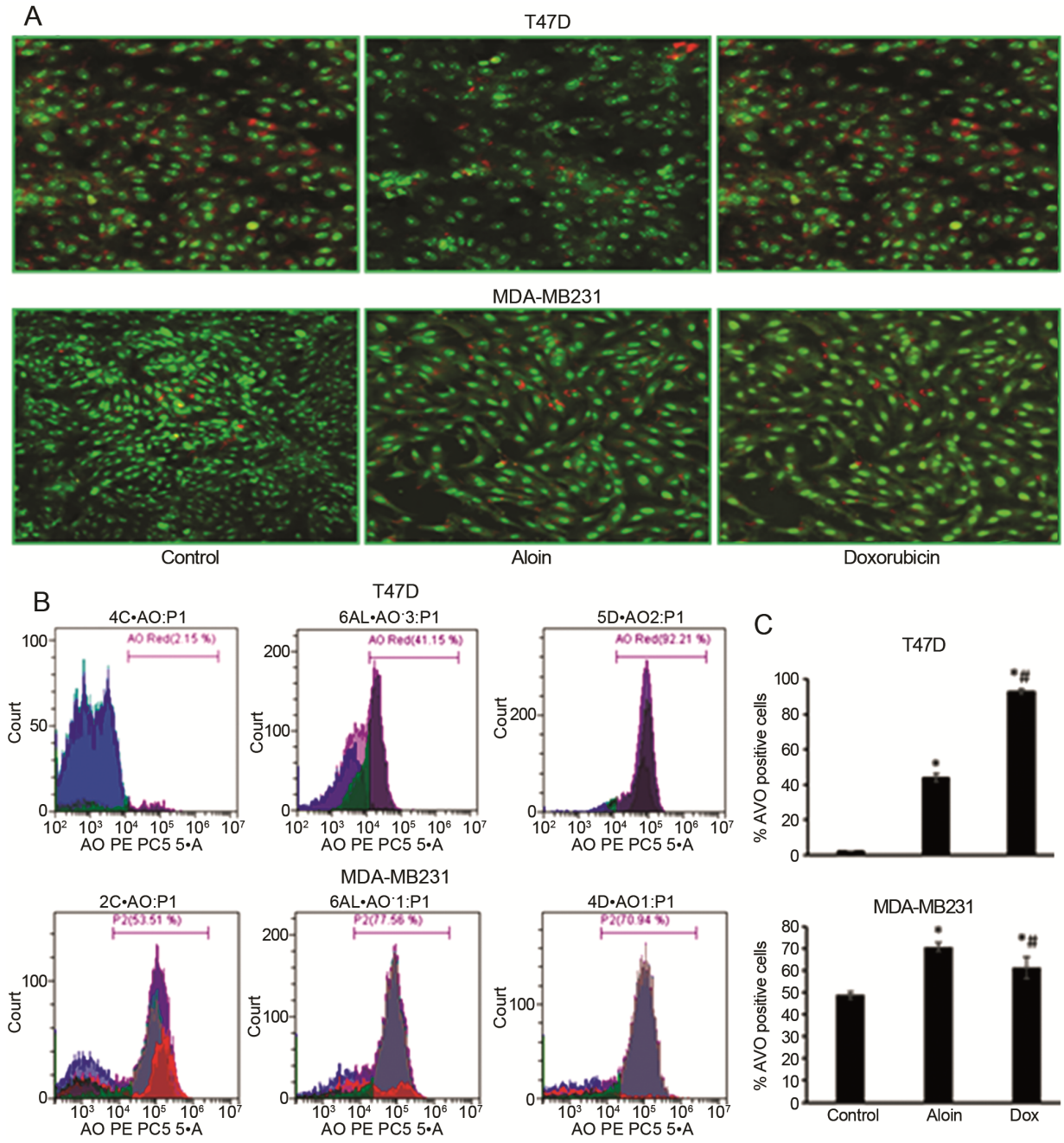

Fig. 5 — Representatives of acridine orange-stained acidic vesicular organelles (AVOs) in response to aloin and Dox treatments. (A) fluorescent micrographs of T47D and MDA-MB231 cells following exposure to aloin (75 and 295 µg/mL, respectively) or Dox (0.1 and 1 µg/mL, respectively) for 72 h. AVOs were visualized using a laser scanning confocal microscope as cells emitting orange/red fluorescence; (B) Flow cytometric analysis of acidic AVOs in treated cells, where light emission in red fluorescence channel (PC5) represents the autophagic cells with AVOs; and (C) Quantitative representation of the percentage of AVOs-positive cells in control and treated cells. [Data are represented as mean±SD of three independent experiments. * denotes significance versus control, while # denotes significance versus aloin-treated cells at P <0.001]

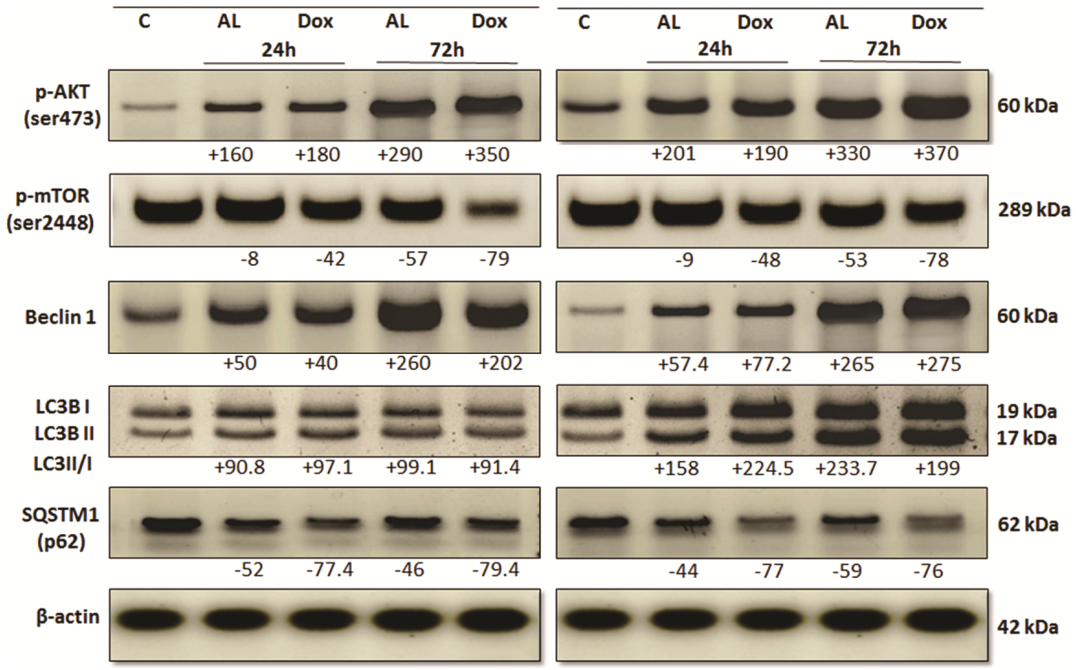

Fig. 6 — Immunoblots of the protein expression of ATG-related genes in breast cancer cells. (A) T47D; and (B) MDA-MB231 cells were treated for the indicated duration with either aloin (75 and 295 µg/mL, respectively) or Dox (0.1 and 1 µg/mL, respectively) then the levels of protein expression of p-AKT, p-mTOR, beclin-1, LC3BI&II, and p62 were detected using Western blot. β-actin was used as a house-keeping protein to normalize the protein expression. Percent change of normalized protein expression was calculated from the densitometric analysis and written underneath each band.

48% for Dox, respectively, and in p62 protein expression (52 and 44%, aloin) and (77.4 and 77%, Dox), respectively, after 24 h exposure. In the 72 h exposure assay, the repression in p-mTOR protein expression reached 57 and 53% for aloin, as well as 79 and 78% for Dox, respectively, while it reached 46 and 59% for aloin as well as 79.41 and 76% for Dox regarding p62 protein expression in T47D and MDA-MB231 tumor cells (Fig. 6).

Discussion

The present study was undertaken to verify the role of aloin in targeting a new molecular mechanism (autophagy) especially in breast tumor cells that suffer from defects in apoptosis-regulatory genes, and its probable contribution to their chemoresistance, compared to Dox as a reference anthraquinone analog. *In vitro* cytotoxicity and clonogenic assays demonstrated that both of ERα+-dependent and ERα+-independent breast cancer cell lines (T47D and MDA-MB231, respectively) were chemosensitive to aloin and Dox in a time- and dose-dependent pattern (Fig. 1 and Table 1). The obtained findings showed that the most prominent effect of aloin is achieved in the prolonged time point (72 h) at all tested concentrations in both subtypes of breast cancer cell lines, which indicates that longer time points are recommended in cells that grow slowly. However, ERα-independent breast tumor cells (MDA-MB23) were more tolerant to aloin than ERα-dependent breast tumor cells (T47D). This is evident by the higher IC_{50} value (4-fold) (Fig. 2). As well, absolute %ICF was obtained in T47D cells in the prolonged exposure regimen at 60 µg/mL, whereas %ICF of 81.58% was recorded at 400 µg/mL in MDA-MB231 tumor cells. Likewise, higher doses of Dox are required to inhibit proliferation of MDA-MB231 cells than T47D cells (10-fold) (Table 1). Rapid growth, hormone independence, and resistance to anticancer agents are part of that phenotype[20]. The mechanistic action of aloin in inhibiting cell proliferation in different cancer cell lines was previously demonstrated. Flow cytometric analysis of breast cancer cells treated with different doses of aloin showed an aneuploidy pattern and a significantly dose-dependent increase in S-phase fraction, and in the proportion of cells cycling at a higher ploidy level (>G2M)[11]. About 18 and 4% of tumor cells contained 2N DNA content, while 16 and 80% of tumor cells contained >4 N DNA content[10]. Furthermore, aloin is recognized as a potent inhibitor of JAK2/STAT3 and JAK2/STAT5a signaling pathway that promotes cell

survival and proliferation[21]. Also, the higher cell growth inhibitory effect of aloin in ERα+T47D cells than in triple negative MDA-MB231 cells might be related to the presence of ERα. In harmony with our suggestion, Kang *et al*.[22] ascribed the increased sensitivity to aloe-emodin treatment in MCF-7 (triple positive cells) than in MDA-MB-231 (triple negative cells) due to the over-expression of ERα in MCF-7 cells. In addition, the lower % cell viability in MCF-7 cell line than in MDA-MB231 cell line after incubation with Dox for 72 h indicates that MDA-MB231 cells were more resistant to Dox treatment[23].

The higher cell growth inhibitory activity of aloin in ERα-dependent breast tumor cells (T47D) in favor of ERα-independent breast tumor cells (MDA-MB231) could also be explained in terms of the study of Huang and co-workers[24]. The authors reported that aloe-emodin (aloin aglucoside) (1,8-dihydroxy-3-hydroxymethyl anthraquinone) inhibits the proliferation of ERα-positive breast cancer cells (MCF-7) by acting as an estrogen receptor modulator that negatively regulates ERα activity by degradation. Aloe-emodin reduces ERα protein levels in both the nuclear and cytosolic fractions, however the impact of aloe-emodin on the cytoplasmic ERα is stronger. This correlates well with ERα proteasome-dependent degradation because of the observed elevation in ubiquitin-conjugated levels. Interestingly, the dissociation of ERα and HSP90 was increased by aloe-emodin treatment, and ERα released from HSP90 protection was subjected to ubiquitination for degradation rather than translocation to the nucleus.

The reasons for chemoresistance are multifaceted and include increased expression of ATP-binding cassette transporters and oncogenes, changes in cell membrane permeability that lead to drug efflux, loss of p53 function, impairment of DNA damage repair mechanisms, epithelial-mesenchymal transition, signal transduction pathways, some epigenetic factors and induction of ATG-mediated drug resistance[25]. However, the concept of ATG as a cytoprotective mechanism can be greatly changed and leads to cellular death (cytotoxic) under certain circumstances. TEM, which is the most reliable method for monitoring ATG[26] was applied to verify the potential role of aloin in activation of ATG process, and the contribution of this process to the increased tolerance of triple negative breast cancer cells to aloin. TEM of T47D and MDA-MB231 cancer cells treated with IC_{50} values of aloin or Dox showed time-dependent double-membraned autophagosomes and autophagolysosomes, as early and late autophagic features, compared to negative control cells (Figs 3 and 4). These findings emphasized ATG as one of the molecular mechanisms used by aloin and Dox to cause cell death in T47D and MDA-MB231 cancer cells.

The aloin-induced ATG in the present study was furtherly corroborated by using acridine orange (AO) staining assay. Acridine orange staining of tumor cells was used to detect the formation of acidic vesicular organelles (AVOs) or late autophagolysosome vacuoles that represent a key feature of late autophagy. The development and distribution of acidic vesicular organelles (AVOs) in ER+ and TN breast tumor cells before and after 72h exposure to aloin or Dox were investigated using laser scanning confocal fluorescence microscopy (Fig. 5).

One important observation is that ERα+T47D control cells showed mainly a green fluorescence (2.1% AVOs), whereas triple negative MDA-MB231 control cells showed green and red fluorescence (48% AVOs), which indicates the presence of high basal level of ATG in metastatic basal-type MDA-MB231 cells than in non-metastatic luminal-type T47D tumor cells. Thus, it could be suggested that ATG is mainly initiated in response to the chemotherapeutic stress in non-metastatic T47D cancer cells (cytotoxic) but constitutes a pro-survival mechanism (cytoprotective) that is provoked in metastatic tumor cells to evade anthracyclines cytotoxicity. In other words, the higher tolerance of MDA-MB231 cells to anthracyclines is likely related to the higher level of ATG. The high basal level of ATG was previously reported as essential to metastatic MDA-MB231 cells for supporting proliferation and matrix invasion[27].

Manipulation of ATG, through stimulation or inhibition, may be viewed as controversial and the choice whether to induce or inhibit ATG is varying and depends on several factors including cell type, concentration and/or time interval, and microenvironment of cultured cells. For instance, Ho and Gorski[28] have recently reported that both ATG process and PI3K/AKT signaling pathway contribute to the resistance of MDA-MB231 tumor cells to anthracyclines. On the contrary, other studies have shown that ATG-related cytotoxicity could be induced in breast cancer cells by exposure to toxic doses of anticancer agents[29,30]. The ATG-induced

cytotoxicity in the previous studies were evidenced by the appearance of ATG characteristics, such as ultrastructural observation of autophagic vacuoles by TEM and the formation of acidic vesicular organelles (AVOs) using acridine orange-staining flow cytometric analysis.

To determine the molecular mechanisms of aloin in ATG initiation, formation, and termination, and to furtherly inquire into the role of autophagy in substantiating the chemosensitivity or chemoresistance of the tested compounds in ERα-dependent (T47D) and ERα-independent breast tumor cells (MDA-MB231), the expression levels of some ATG-related proteins were studied. The role of AKT/mTOR signaling involved in anthracyclines-mediated ATG in both types of breast cancer cell lines was evaluated in the present study. Western immunoblotting revealed a time-dependent increase in the relative protein expression level of p-AKT gene, and conversely a downregulation in p-mTOR protein expression in both types of breast cancer cells following exposure to aloin and Dox. It is noteworthy that the extent of overexpression of p-AKT protein, but not p-mTOR, was more notable in Dox treatment and in MDA-MB231 tumor cells. The inhibition of p-mTOR protein expression combined with TEM and FACS findings indicate that both aloin and Dox act at early stages of ATG. The over-expression of p-AKT protein is elusory and needs further research. It implicates that aloin/Dox-potentiated ATG in breast cancer is AKT independent, and thus excludes the possible negative regulation of AKT activity. It might also be due to insufficiency of the tested drugs. Another plausible suggestion that warrants further investigation is that both aloin and Dox mimic the actions of rapamycin and its analogs (rapalogs) as selective inhibitors of mTOR, that inhibit the mTOR downstream activity by limiting phosphorylation of p70S6K and the translational repressor; eukaryotic translation initiation factor 4E binding protein 1(4EBP1), resulting in p-Ser473-AKT activation[31]. As well, assessment of the upstream p-PI3K activity is required because co-treatment of aloin and a PI3K inhibitor (such as LY294002) could suppress the activity of the PI3K/AKT/mTOR axis and mitigate the p-AKT (Ser473) activation feedback loop in both cell lines. The increased relative expression of beclin 1 protein, a vesicle formation indicator, was greatly enhanced in both breast cancer cell lines (3.5- to 5-fold) in the prolonged exposure, indicating a highly activated ATG.

The proceeding of ATG machinery was verified by determining the expression of microtubule-associated protein 1 light chain 3 beta proteins (LC3BI&II) and their ratio (LC3II/LC3I), reliable autophagosome formation markers. Results revealed an increase in the relative protein expression of both LC3I and LC3II genes, as well as their ratio (LC3II/LC3I) in both types of breast cancer cells following aloin and Dox treatment with variable degrees. However, the enhanced effect was noticed in triple negative MDA-MB231 cells in the prolonged treatment, which parallel the formation of autophagosomes and ATG vacuoles (Fig. 4). Several studies reported the overexpression of LC3I and LC3II and their ratio after treatment with different therapeutic agents[32,33]. A relevant study conducted by Lee *et al*.[34] demonstrated that aloin treatment (100 μM) consistently induced expression of LC3II protein in human lung cancer cell line (A549). Recently, Sun *et al*.[35] reported that aloin inhibits the growth and invasion of hepatocellular carcinoma cells (HepG2) by increasing the relative protein expression levels of autophagosome markers including, beclin-1, LC3II and ATG8 (a ubiquitin-like protein). However, in mammalian cells the total level of LC3 does not necessarily change in a predictable manner, as there may be increases in the conversion of LC3I to LC3II or a decrease in LC3II relative to LC3I if degradation of LC3II via lysosomal turnover is particularly rapid. Both of these events can be seen sequentially in several cell types as a response to total nutrient and serum starvation[36]. This explanation accounts for the decreased expression level of LC3II relative to LC3I in tumor cells exposed to either aloin or Dox in both ERα+ T47D and triple negative MDA-MB231 tumor cells. Maxwell *et al*.[37] found that phytoestrogen, arctigenin (a biologically active lignan, isolated from *Arctium lappa*, Asteraceae family) mainly targeted the mTOR pathway in triple positive MCF7 breast cancer cells, leading to ATG-induced cell death accompanied with increased expression in both LC3 protein types along with the ratio of LC3II/LC3I. The authors demonstrated that, similar to arctigenin, treatment with rapamycin also inhibited ERα protein expression, suggesting that mTOR inhibition could lead to decreased ERα protein expression, probably due to inhibition of protein synthesis.

To exclude that accumulation of LC3 was due to inhibition, rather than induction of ATG, the sequestosome-1(SQSTM1)/p62 protein expression, as

a marker of activated autophagic flux was also determined. Since p62 itself is removed mainly by ATG, its amount is generally considered to inversely correlate with the autophagic flux[38]. Results obtained from the present study revealed a degradation of p62 manifested by moderate repression in the protein expression of p62 gene in T47D and MDA-MB231 tumor cells exposed to aloin at the two time points, which was augmented in Dox treatment. This confirms that the effects of both aloin and Dox continue at later stages of ATG, promoting the fusion of auto-phagosomes and lysosomes, thereby enhancing the autophagic flux. In accordance with our findings, aloin treatment (50 μmol/L) was previously reported to reduce the p62 protein expression in hepatocellular carcinoma cells (HepG2 and Bel-7402 cells) after 48h[36]. Also, a remarkable degradation of p62 in ERα+ breast cancer cells (MCF7 and T47D) exposed to sunitinib (a tyrosine kinase inhibitor) was recorded indicating increased autophagic flux[39]. In addition, Aydinlik *et al.*[40] studied whether or not autophagy played a role in treatment of triple negative breast cancer (MDA-MB231) with Dox, and demonstrated a marked increase in LC3II/LC3I ratio and reduction in p62 protein expression upon treatment with Dox (0.46-1.84 μM).

Conclusion

Our results show that the triple negative breast tumor cells are less sensitive to aloin and Dox than ERα+ breast tumor cells, and that the variant drug response to anthracyclines is cell type- and time-dependent. The high tolerance of triple negative breast tumor cells to aloin and Dox than ERα+ breast tumor cells is due to enhancement of pre-formed ATG independent of AKT signaling. Aloin/Dox-promoted ATG could be considered as an effective alternative mechanism for cell death in ERα+breast cancers with deficient or mutant p53. Also, being inhibitor of mTOR, a serine/threonine kinase and the tyrosine kinase JAK2, as previously reported, highlighted the important role of aloin as a multi-kinase inhibitor.

Conflict of interest

Authors declare no competing interests.

References

1 Siegel RL, Miller KD, Wagle NS & Jemal A, Cancer statistics, 2023. *CA: a cancer journal for clinicians*, 73 (2023) 17.

2 Nedeljković M & Damjanović A. Mechanisms of chemotherapy resistance in triple-negative breast cancer-how we can rise to the challenge. *Cells*, 8 (2019) 957.

3 Ramirez JAZ, Romagnoli GG & Kaneno RJLS, Inhibiting autophagy to prevent drug resistance and improve anti-tumor therapy. *Life Sci*, 265 (2021) 118745.

4 Xiang Y, Zhao J, Zhao M & Wang K, Allicin activates autophagic cell death to alleviate the malignant development of thyroid cancer. *Exp Ther Med*, 15 (2018) 3537.

5 Ravindra Wagh U & Rupachandra S, New insights of RA-V cyclopeptide as an autophagy inhibitor in human COLO 320DM cancer cell lines. *Indian J Biochem Biophys*, 58 (2021) 426.

6 Khan A, Singh VK, Thakral D & Gupta R. Autophagy in acute myeloid leukemia: a paradoxical role in chemoresistance. *Clin Transl Oncol*, 24 (2022) 1459.

7 Sánchez M, González-Burgos E, Iglesias I & Gómez-Serranillos MP, Pharmacological update properties of *Aloe vera* and its major active constituents. *Molecules*, 25 (2020) 1324.

8 Manirakiza A, Irakoze L & Manirakiza S, Aloe and its Effects on Cancer: A Narrative Literature Review. *East Afr Health Res J*, 5 (2021) 1.

9 Fahim FA, Abd-Allah NM, Ela F & Esmat A, Aloin: A natural anthraquinone with potential antitumour activity. *J Tumor Marker Oncol*, 8 (1993) 27.

10 Fahim FA, Esmat AY, Mady EA & Amin MA, Serum LDH and ALP isozyme activities in mice bearing solid Ehrlich carcinoma and/or treated with the maximum tolerated dose (MTD) of aloin. *Dis Markers*, 13 (1997) 183.

11 Fahim FA, Abd-Allah NM & Esmat AY, Some metabolic aspects in normal and tumour-bearing mice treated with a natural anthraquinone. *J Tumor Marker Oncol*, 8 (1993) 35.

12 Esmat AY, El-Gerzawy SM & Rafaat A, DNA ploidy and S phase fraction of breast and ovarian tumor cells treated with a natural anthracycline analog (aloin). *Cancer Biol Ther*, 4 (2005) 108.

13 Esmat AY, Tomasetto C & Rio MC, Cytotoxicity of a natural anthraquinone (Aloin) against human breast cancer cell lines with and without ErbB-2: topoisomerase IIalpha coamplification. *Cancer Biol Ther*, 5 (2006) 97.

14 Esmat AY, Said MM, Hamdy GM, Soliman AA & Khalil SA, *In vivo* and *in vitro* studies on the antioxidant activity of aloin compared to doxorubicin in rats. *Drug Develop Res*, 73 (2012) 154.

15 Esmat AY, Said MM & Khalil SA, Aloin: a natural antitumor anthraquinone glycoside with iron chelating and non-atherogenic activities. *Pharm Biol*, 53 (2015) 138.

16 Marks DC, Belov L, Davey MW, Davey RA & Kidman AD, The MTT cell viability assay for cytotoxicity testing in multidrug-resistant human leukemic cells. *Leuk Res*, 16 (1992) 1165.

17 Bradford MM, A rapid and sensitive method for the quantitation of microgram quantities of protein utilizing the principle of protein-dye binding. *Anal Biochem*, 72 (1976) 248.

18 Laemmli UK, Cleavage of structural proteins during the assembly of the head of bacteriophage T4. *Nature*, 227 (1970) 680.

19 Shapiro SS & Wilk MB, An analysis of variance test for normality (complete samples). *Biometrika*, 52 (1965) 591.

20 Kim RK, Suh Y, Yoo KC, Cui YH, Kim H, Kim MJ, Kim IG & Lee SJ, Activation of KRAS promotes the mesenchymal features of basal-type breast cancer. *Exp Mol Med*, 47(2015) e137.

21 Muto A, Hori M, Sasaki Y, Saitoh A, Yasuda I, Maekawa T, Uchida T, Asakura K, Nakazato T, Kaneda T, Kizaki M, Ikeda Y & Yoshida T, Emodin has a cytotoxic activity against human multiple myeloma as a Janus-activated kinase 2 inhibitor. *Mol Cancer Ther*, 6 (2007) 987.
22 Kang SC, Lee CM, Choung ES, Bak JP, Bae JJ, Yoo HS, Kwak JH & Zee OP, Anti-proliferative effects of estrogen receptor-modulating compounds isolated from Rheum palmatum. *Arch Pharm Res*, 31 (2008) 722.
23 Georgiev KD, Slavov IJ & Iliev IA, Synergistic growth inhibitory effects of *Lycium barbarum* (Goji berry) extract with doxorubicin against human breast cancer cells. *J Pharm Pharmacol Res*, 3 (2019) 51.
24 Huang PH, Huang CY, Chen MC, Lee YT, Yue CH, Wang HY & Lin H, Emodin and Aloe-Emodin Suppress Breast Cancer Cell Proliferation through ER α Inhibition. *Evid Based Complement Alternat Med*, 2013 (2013) 376123.
25 Tendulkar S & Dodamani S, Chemoresistance in ovarian cancer: prospects for new drugs. *Anticancer Agents Med Chem*, 21 (2021) 668.
26 Mizushima N, Methods for monitoring autophagy. *Int J Biochem Cell Biol*, 36 (2004) 2491.
27 Tyutyunyk-Massey L & Gewirtz DA, Roles of autophagy in breast cancer treatment: Target, bystander or benefactor. *Semin Cancer Biol*, 66 (2020) 155.
28 Ho CJ & Gorski SM, molecular mechanisms underlying autophagy-mediated treatment resistance in cancer. *Cancers*, 11 (2019) 1775.
29 Gao S, Li X, Ding X, Qi W & Yang Q, Cepharanthine induces autophagy, apoptosis and cell cycle arrest in breast cancer cells. *Cell Physiol Biochem*, 41 (2017) 1633.
30 Lee WY, Hsu KF, Chiang TA & Chen CJ, *Phellinus linteus* extract induces autophagy and synergizes with 5-fluorouracil to inhibit breast cancer cell growth. *Nutr Cancer*, 67 (2015) 275.
31 Oshiro N, Yoshino K, Hidayat S, Tokunaga C, Hara K, Eguchi S, Avruch J & Yonezawa K, Dissociation of raptor from mTOR is a mechanism of rapamycin-induced inhibition of mTOR function. *Genes Cells*, 9 (2004) 359.
32 Bao L, Jaramillo MC, Zhang Z, Zheng Y, Yao M, Zhang DD & Yi X. Induction of autophagy contributes to cisplatin resistance in human ovarian cancer cells. *Mol Med Rep*, 11 (2015) 91.
33 Xue L, Zhang WJ, Fan QX & Wang LX. Licochalcone A inhibits PI3K/Akt/mTOR signaling pathway activation and promotes autophagy in breast cancer cells. *Oncol Lett*, 15 (2018) 1869.
34 Lee M-C, Liao J-D, Huang W-L, Jiang F-Y, Jheng Y-Z, Jin Y-Y & Tseng Y-S. Aloin-induced cell growth arrest, cell apoptosis, and autophagy in human non-small cell lung cancer cells. *Biomark Genom Med*, 6 (2014) 144.
35 Sun R, Zhai R, Ma C & Miao W, Combination of aloin and metformin enhances the antitumor effect by inhibiting the growth and invasion and inducing apoptosis and autophagy in hepatocellular carcinoma through PI3K/AKT/mTOR pathway. *Cancer Med*, 9 (2020) 1141.
36 Klionsky DJ, Abdalla FC, Abeliovich H, Abraham RT, Acevedo-Arozena A & Adeli K, Guidelines for the use and interpretation of assays for monitoring autophagy. *Autophagy*, 12 (2016) 1.
37 Maxwell T, Lee KS, Kim S & Nam KS, Arctigenin inhibits the activation of the mTOR pathway, resulting in autophagic cell death and decreased ER expression in ER-positive human breast cancer cells. *Int J Oncol*, 52 (2018) 1339.
38 Zhang Z, Rui W, Wang ZC, Liu DX & Du L, Anti-proliferation and anti-metastasis effect of barbaloin in non-small cell lung cancer via inactivating p38MAPK/Cdc25B/Hsp27 pathway. *Oncol Rep*, 38 (2017) 1172.
39 Abdel-Aziz AK, Shouman S, El-Demerdash E, Elgendy M & Abdel-Naim AB, Chloroquine synergizes sunitinib cytotoxicity via modulating autophagic, apoptotic and angiogenic machineries. *Chem Biol Interact*, 217 (2014) 28.
40 Aydinlik S, Erkisa M, Cevatemre B, Sarimahmut M, Dere E, Ari F & Ulukaya E, Enhanced cytotoxic activity of doxorubicin through the inhibition of autophagy in triple negative breast cancer cell line. *Biochim Biophys Acta*, 1861 (2017) 49.